EUROPEAN ORGANIZATION FOR NUCLEAR RESEARCH

CERN-SR
26 April 2023

NP04 2023 Annual Report to the CERN-SPSC

The ProtoDUNE NP04 collaboration

Abstract
NP04 2023 Annual Report to the CERN-SPSC

CERN-SPSC-2023-017 / SPSC-SR-330
27/04/2023

Contents

1 NP04 Phase-I: Beam/cosmic Data Analysis . . . 2
1.1 Publication status . . . 2
1.2 Hadron–Ar Cross Sections . . . 2
1.3 Other TPC analyses . . . 6
1.4 Analysis of photon detectors data . . . 8
2 Status and plans for NP04 phase-II . . . 9
2.1 NP04 Installation and preparation for filling . . . 9
2.2 Status and plans for commissioning and calibration . . . 13
2.3 Plans and Schedule for operation . . . 14
3 Summary . . . 15

1 NP04 Phase-I: Beam/cosmic Data Analysis

1.1 Publication status

Since the Spring 2022 report the paper [1] describing the convolutional neural network used for tagging hits as either track-like, shower-like or from Michel electrons was published. Two other papers have been posted to the arXiv and are in journal review: the Michel electron analysis is under consideration in PRD [2] and the responses to a second round of comments have been completed, and the Pandora event reconstruction software performance paper has been through the first round of comments in EPJC [3]. Two other analyses have completed the ProtoDUNE working group review process and are now under review by the DUNE analysis review committees: measurements of the exclusive π^+–Ar cross sections and the K^+-Ar inelastic cross section, described in sections 1.2.2 and 1.2.4, respectively. The cosmic ray seasonal variation analysis is in ProtoDUNE working group review, and described in section 1.3.2.

1.2 Hadron–Ar Cross Sections

The primary physics goals for ProtoDUNE-SP are the measurement of hadron interaction cross sections on liquid argon. In this section we review the status of the different analyses and present the plans for the coming year.

1.2.1 Inclusive π^+–Ar inelastic cross section

Based on the idea of the thin-slice method proposed by the LArIAT collaboration [4], we further developed the method and provide with an energy-slicing method without the thin-target assumption. To use this method, we need to measure the initial energy as well as the final energy of the beam track reconstructed inside the TPC. In order to correct some known differences between data and MC, we reweight the muon fraction of the beam and the beam momentum in the simulation. After full selections, the purity of pion inelastic events is over 80%, estimated by the reweighted MC sample. After that, we use a data-driven sideband fit to subtract the remaining backgrounds. Finally, multi-dimensional unfolding is implemented, considering full constraints between the measured initial energy and the final energy from the beam tracks. The preliminary cross-section results using the 1 GeV/c beam data are given in Figure 1, including most systematic uncertainties. A detailed analysis note is in preparation. The 2 GeV/c and 3 GeV/c pion analyses are ongoing, following the same procedures, but with different selection conditions.

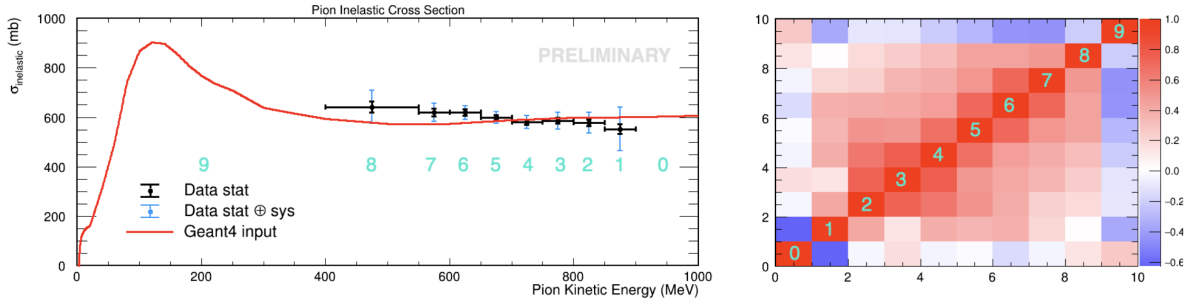

Figure 1: Left: preliminary results of the pion-argon inelastic cross-section measurement using 1 GeVc data (black points) compared to the G4 prediction (red). Right: the correlation matrix between energy bins.

1.2.2 Exclusive π^+–Ar cross sections

In addition to the total inelastic π^+–Ar cross section measurement described above, a measurement of exclusive channels is also in progress and nearing completion. This measurement will be useful for 1) constraints of the rate of secondary π^+–Ar interactions of π^+ emitted from ν–Ar interactions and 2) constraints of "Final State Interaction" (FSI) models within ν–Ar event generators. This will improve the accuracy of DUNE's simulation and help achieve its tight systematic uncertainty budget.

A likelihood-fit-based analysis has been developed for the simultaneous measurement of the three inelastic cross-section "channels": absorption (zero pions of any charge in the final state), charge exchange (π^0s and no charged pions in the final state), and "other" (any other type of inelastic interaction) [5]. The fit varies the number of true π^+–Ar interactions of the three channels in MC as well as a parameter controlling the relative number of beam μ^+ and a set of systematic parameters, and compares the resulting event rate predictions to data. The cross sections are extracted from truth information of the best-fit MC using the previously mentioned thin-slice method. This is repeated for an ensemble of statistical throws according to the parameter covariance matrix resulting from the fit in order to determine the covariance of the cross sections. An internal review of the analysis has been completed, and internal publication procedures have begun. Figures 2(a) and 2(b) show the preliminary results of the extracted cross sections for absorption and charge exchange compared to Geant4 v10.6. Figure 2(a) also includes a comparison to lower-energy π^+–Ar absorption results from the LADS collaboration [6]

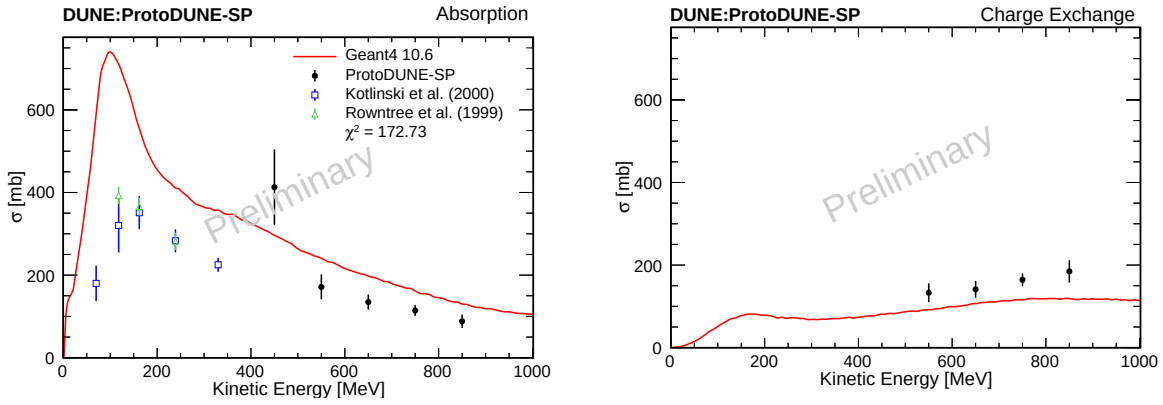

(a) (b)

Figure 2: Preliminary exclusive cross section results from likelihood-fit based analysis (black circles) compared to Geant4 v10.6 predictions (red curves) and a measurement of π^+–Ar absorption by the LADS collaboration (blue open squares [7] and green open triangles [6]).

1.2.3 p-Ar inelastic cross section

Neutrino event generators are essential in the field of neutrino oscillation physics, providing predictions for final state particle distributions and energy spectra in neutrino-nucleus interactions. Accurate modeling of final state interactions (FSI) in these generators is crucial to obtain precise measurements of neutrino oscillation parameters, as FSI represents the main source of systematic uncertainty [8]. Although many theoretical predictions of p-Ar inelastic cross sections from various neutrino event generators exist [9], there are only a few measurements. In this analysis, we aim to test these predictions using ProtoDUNE-SP 1 GeV/c proton data. Our ultimate objective is to improve our understanding of FSI modeling and reduce systematic uncertainties in neutrino-argon interactions.

Figure 3 presents preliminary results of the p-Ar inelastic cross section using all ProtoDUNE-SP 1 GeV/c data. The analysis considered several systematic uncertainties, including the impact of uncertainties in the I-value in Bethe-Bloch dE/dx calculation highlighted in a recent study [10] and uncertainties of beam momentum reweighting. Background systematics were evaluated using background-rich samples to measure the variations and assess their impacts on the cross section. The preliminary results show reasonable agreement with Geant4 and demonstrated the ability to measure the cross section at low energy. The current work is focused on refining the results, finalizing the systematics, and preparing the technical note. We expect the entire analysis to be completed this year and undergo internal reviews before the results are published.

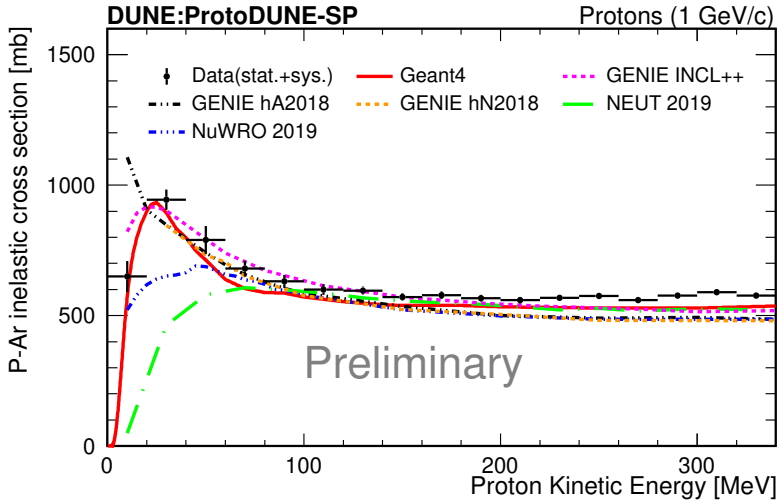

Figure 3: Preliminary results of the proton-argon inelastic cross section measurement using 1 GeV/c data. The black points represent the reconstructed cross section using the E-slice method, and the Geant4 prediction is shown in red curve. Various other predictions from different neutrino event generators [9] are shown for comparison.

We are also conducting an analysis at 2 GeV/c using a similar technique. The event selection cuts have been developed and achieved 80 % purity. Our goal for this year is to deliver preliminary physics results. Finally, we have recently started the analysis of the p-Ar inelastic cross section at 3 GeV/c. These analyses will expand our understanding of the energy dependence of the cross section at higher energies.

1.2.4 K-Ar inelastic cross section

The ProtoDUNE-SP test beam provided primary kaons at momentum settings of 6 GeV/c and 7 GeV/c. The analysis measures a total inelastic cross section using the LArIAT method of thin slices [4, 11]. This type of analysis divides the detector into small slices based on the collection plane wire that would detect

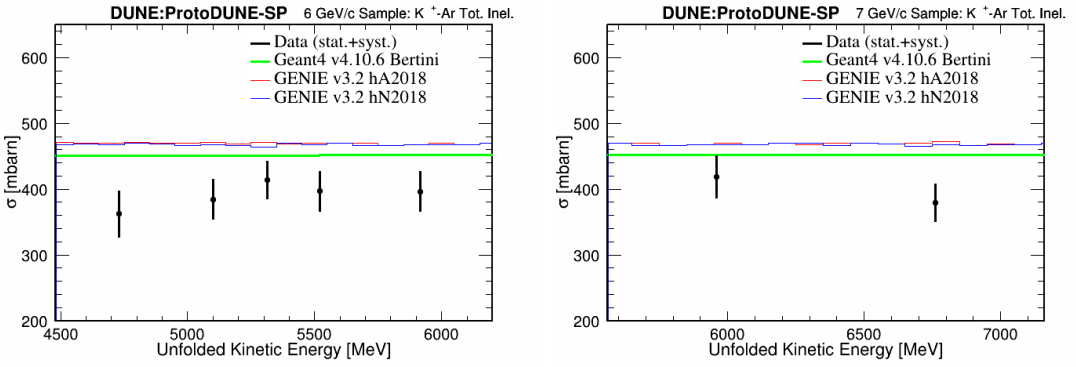

Figure 4: Total inelastic cross section measured from primary beam kaons with test beam data taken at the 6 GeV/c setting (left) and 7 GeV/c (right). Comparisons included on the measured cross section are to the simulations GENIE v3.2.0 and Geant4 [17–24].

signals from the slice. Between these smaller volumes, the kaon travels across the detector's length, and either moves to the next slice or interacts within the slice. The ratio of incident and interacting slices measured then is used to measure the cross section based on classical physics formulas for the survival probability of a particle with a mean free path traveling a distance in a medium.

Due to detector distortions, the reconstruction can miss slices from the truth-level information in the simulation. The missed slices could be because the whole primary beam kaon was not selected as a good kaon candidate or because a specific slice was missed due to inefficiencies in the reconstruction and identification of an interacting kaon. RooUnfold was used to compensate for these effects and uses Bayesian-like unfolding to handle the smearing of the energy measurements from the detector response and the efficiency corrections necessary to recover slices missed by the reconstruction [12, 13]. These steps ensure that the unfolding process can extract the underlying model used in the simulation through four iterations on both the incident and interacting distributions. Systematic uncertainties involve altering the fraction of events missed by the test beam reconstruction, tuning the number of events that pass the fiducial volume, and smearing the measured kinetic energy used in the unfolding process caused uncertainty on dE/dx and the uncertainty on the beam momentum measurement modeling [14, 15].

The changes made in the past year include the usage of the full 6 GeV/c and 7 GeV/c samples, rebinning of the analysis for uniform statistical uncertainties, the addition of a Geant4 modeling uncertainty [16], and the tuning of the uncertainties based on further information on reconstruction performance [3]. Figure 4 shows the preliminary results for the total inelastic kaon cross section.

1.2.5 Differential π-Ar charge exchange cross section

In this study, we aim to measure the cross-section in the pion-argon charge exchange (CEX) channel. This channel is characterized by the presence of a well-reconstructed π^0 particle and no other mesons in the final state. We utilized a modified energy-slice method to extract the cross-section by counting the incident and interacting flux. We selected 665 candidate signal events (from a sample of 34,783 1 GeV/c pion beam events) with a purity of 70% based on the MC simulation. We employed two sideband channels to tune the pion production background.

The preliminary total CEX cross-section results are presented in the left plot in Fig. 5. This analysis is currently limited by the statistics due to the low efficiency of reconstructing two π^0 showers. Additionally, the differential cross-section measurement of beam pions interacting with energies ranging from 650-800 MeV has been conducted, with a particular emphasis on the produced π^0 kinematics. The results are shown as a function of the π^0 kinetic energy in the right plot of Fig. 5, and a measurement as a function of the angle of the π^0 with respect to the π^+ was also made. The "three-peak" structure

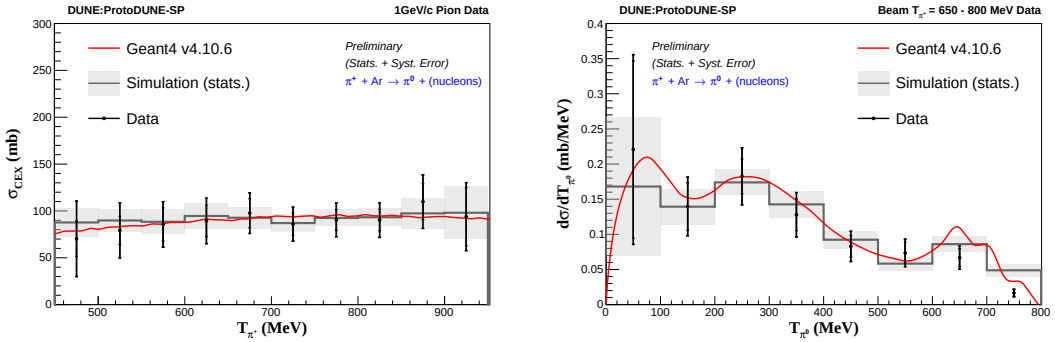

Figure 5: Left: the total pion-argon charge exchange cross-section preliminary result in energy between 450 - 950 MeV. Right: the differential charge-exchange cross section as a function of the π^0 kinetic energy.

in the kinetic energy cross-section distribution is a result of the different π^0 kinematics that arise from producing many, few, and very few nucleons/nuclei in the final state. Our measurements help reduce the uncertainties associated with π–Ar interactions and can aid in the improvement of models currently used in neutrino event generators and detector simulation packages.

1.3 Other TPC analyses

1.3.1 Diffusion

As clusters of ionization electrons drift in the electric field of an LArTPC, their motion is impacted by diffusion. Longitudinal electron diffusion, occurring parallel to the electric field, is theorized to have a smaller effect on electron spread than transverse electron diffusion, which occurs perpendicular to the electric field [25]. Both processes contribute to systematic uncertainties on charge and energy resolution in LArTPCs. Longitudinal electron diffusion has been measured in liquid argon previously at various electric fields [26–30], but additional measurements at electric fields relevant to DUNE are important to alleviate tension between these existing measurements. Transverse electron diffusion, having never been measured directly in an LArTPC, is essential to characterize before DUNE turns on.

The primary measurable quantity sensitive to electron diffusion is the shape of the signal pulse created from charge collection on a wire. Signal pulses include Gaussian contributions from both longitudinal and transverse diffusion which are dependent on electron drift time from the ionization point to the anode. The transverse diffusion component is also dependent on the angle θ_{XZ} made by the track from which the ionization event originated and the direction perpendicular to both the drift direction and the collection wire orientation. Signal pulses also include a boxcar-shaped contribution which depends on $|\theta_{XZ}|$ and the collection wire pitch. The independent pulse widths corresponding to these two Gaussian and one boxcar contribution are shown as functions of drift time and/or $|\theta_{XZ}|$ in Figure 6. Based on the projected magnitudes of these contributions, we determined that ProtoDUNE-SP has the sensitivity required to simultaneously measure longitudinal and transverse electron diffusion through analysis of signal pulse widths. Development of this analysis is ongoing.

Additionally, we are in the process of measuring longitudinal diffusion independently from transverse diffusion at the four different electric field strengths at which ProtoDUNE-SP took cosmic ray muon data: 350 V/cm, 500 V/cm, 600 V/cm, and 650 V/cm. This analysis only uses tracks with low $|\theta_{XZ}|$ so as to isolate longitudinal diffusion's effect on the pulse width.We plan to finalize and publish these measurements within this calendar year.

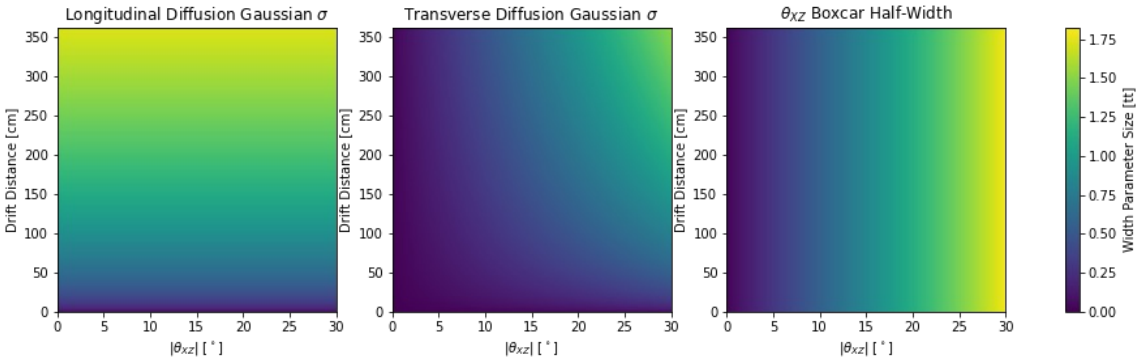

Figure 6: Significant contributions to hit pulse width from physical sources occur as functions of drift distance and/or $|\theta_{XZ}|$ angle. Width parameters are quantified in time ticks (tt), where one time tick corresponds to 0.5 microseconds.

1.3.2 Seasonal variation of cosmic ray muon rate

Utilizing cosmic muons as a standard candle is a highly effective technique, as it provides a calibrated and stable reference signal that allows us to evaluate detector performance and understand its response but also for physics measurements. It is well-known that the fluxes of cosmic ray muons observed in underground or surface detectors exhibit a seasonal variation [31–35].

A set of cosmic runs were selected when the detector was running with stable conditions. Selection criteria were then used in order to reject delta rays and poorly reconstructed tracks. The selection was compared between data and simulation and was found to be in good agreement, as shown in the cosmic track length distribution on the left of Fig 7. Although the simulation is not used in the analysis, detailed comparisons were performed between data and simulation to serve as basic sanity checks.

We estimate the cosmic muon rate for each cosmic run using the mean number of tracks per event, and the event time window. The right plot in Fig. 7 shows the measured cosmic muon rate as a function of day in a year interval, fit by a sinusoidal function of the form:

$$g(t) = C * \left(1 + B * \cos\left[\frac{2\pi}{P}(t - t_0)\right]\right)$$

where C is the absolute muon rate, B is the fractional modulation amplitude, P is the period which is set at 365 days, t_0 is the day of the maximum muon rate, and t is the number of days elapsed since Jan. 1. The parameters C, B, t_0 are free to float in the fit. The seasonal variation is clear and measured at the 3 sigma level : the muon rate is lower in the summer and higher in the winter as expected. The fitted amplitude is 4.8 ± 1.6% and the maximum muon rate is observed in February, 40 ± 12 days, which is in good agreement with the measurements from other surface experiments [31, 33].

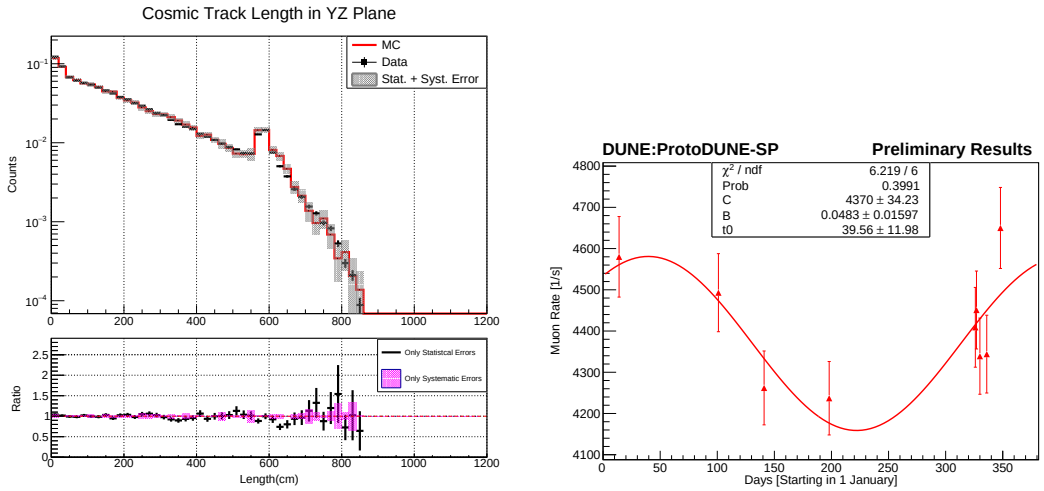

Figure 7: Left: the cosmic muon track length distribution. Right: the measured seasonal variation of the cosmic muon rate.

1.3.3 Hypothetical track length fitting

Energy measurement of interacted secondary charged hadrons is important for ProtoDUNE hadron cross section analyses as well as neutrino experiments based on LArTPCs. We are developing a new energy measurement method called the hypothetical track-length fitting method. The method fits for the best additional track length using the residual range and dE/dx of hits from reconstructed tracks.

We are considering two methods to find the best additional track length. First method is minimizing the χ^2 between dE/dx of hits and expected dE/dx coming from the Bethe-Bloch formula. The other method is maximizing likelihood using the Vavilov distribution as the probability density function of dE/dx values. To save CPU time, the Vavilov function is approximated into Gaussian and Landau distribution for very large and small number of ionizing interactions per unit length, respectively. Performance of the hypothetical track-length fitting method based on the maximum likelihood is being tested using stopped charged pions. In this case, the range-based energy can be used as reference.

Before studying the energy measurement performance using the range-based energy, a study using the MC truth energy was done using ProtoDUNE-SP 1 GeV/c beam MC sample and showed the resolution is better than 6% and fractional bias is smaller than 4%. The energy measurement performance using the range-based energy was performed using the event reconstruction and a comparison between ProtoDUNE-SP 1 GeV/c beam data and MC samples is shown in Fig 8. The study to identify systematic uncertainties is ongoing. Our goal is providing a general method for assigning systematic uncertainties to energy scale and resolution of the hypothetical track-length fitting method that any LArTPC data analyzer can follow. We aim to publish this work in JINST as a DUNE collaboration paper.

1.4 Analysis of photon detectors data

The analysis of the Xe-doping run (see 2022 Annual Report) has been completed and the draft publication is currently under Collaboration review. The analysis has shown that doping up to 16 ppm can be safely accomplished without jeopardizing the charge collection and was effective to recover the loss of scintillation light due to nitrogen contamination. Fig. 9 shows the average waveform of a standalone X-ARAPUCA sensitive to Ar+Xe light (top) and of an ancillary X-ARAPUCA sensitive to Xe light only (bottom) as a function of the xenon concentration. Besides the use of the standalone X-ARAPUCA, the full analysis demonstrates light recovery through the attenuation curves after xenon injection with the non-beam side PDS ARAPUCA.

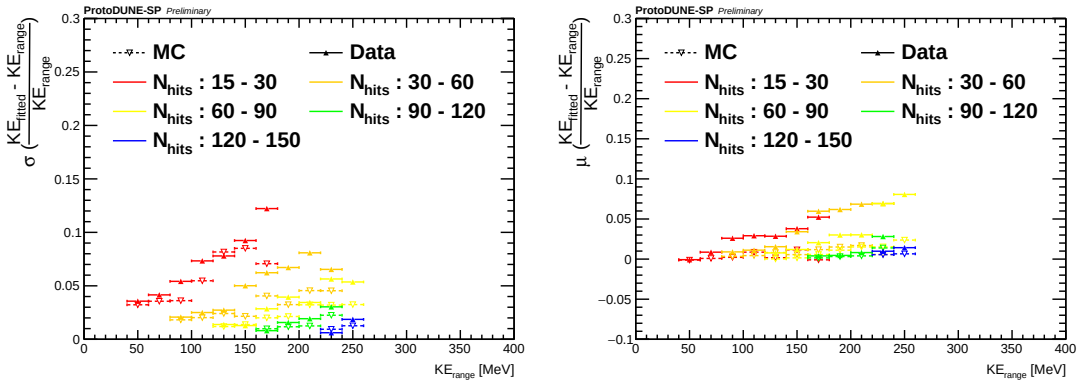

Figure 8: Summarized plots of energy measurement performance of the hypothetical track-length fitting method based on maximum likelihood method. Resolutions (left) and fraction biases (right) are shown as functions of charged pions' range-based kinetic energy and number of hits. Pure secondary charged pions are selected from the MC sample.

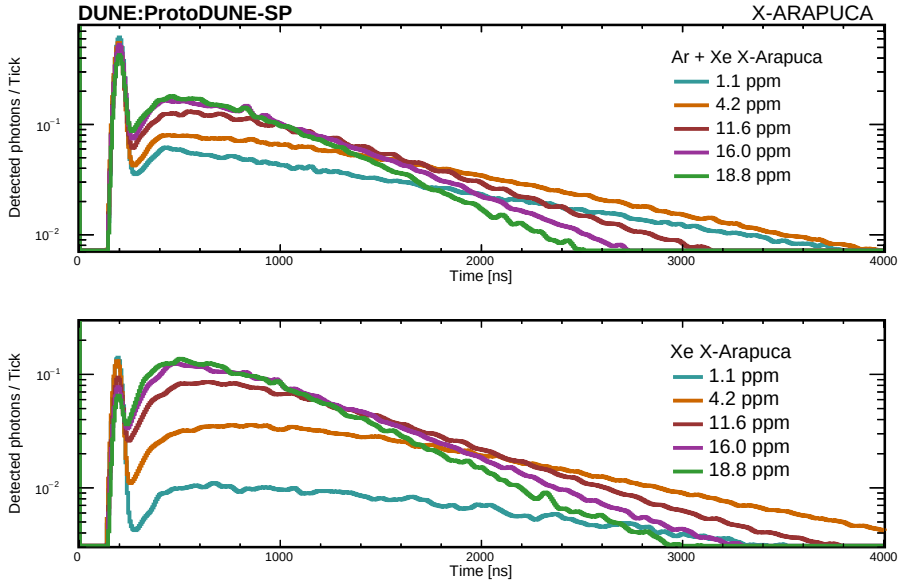

Figure 9: Average waveforms obtained after deconvolution of single photoelectron pulse, at different stages of xenon doping (after nitrogen pollution). Data from runs with no electric field. Top panel: The Ar+Xe-light sensitive X-ARAPUCA; bottom panel: the Xe-light-only sensitive X-ARAPUCA. Only events with at least three detected photons in the Ar+Xe X-ARAPUCA module are selected.

2 Status and plans for NP04 phase-II

2.1 NP04 Installation and preparation for filling

The installation of the LAr-TPC components of ProtoDUNE NP04 was essentially concluded in 2022.

All four APAs, integrated with the cold electronics, were tested at cold with N2 gas at 180 K and have confirmed their excellent performance in terms of noise: the design goal of less than 1000 electrons ENC at cold for all channels, was achived for all APAs (see Fig. 10). APAs are now installed in the cryostat in their final position. The CE cables have been pulled through cryostat penetration and connected to the warm part of the electronics via the cryostat feedthroughs (see Fig. x2).

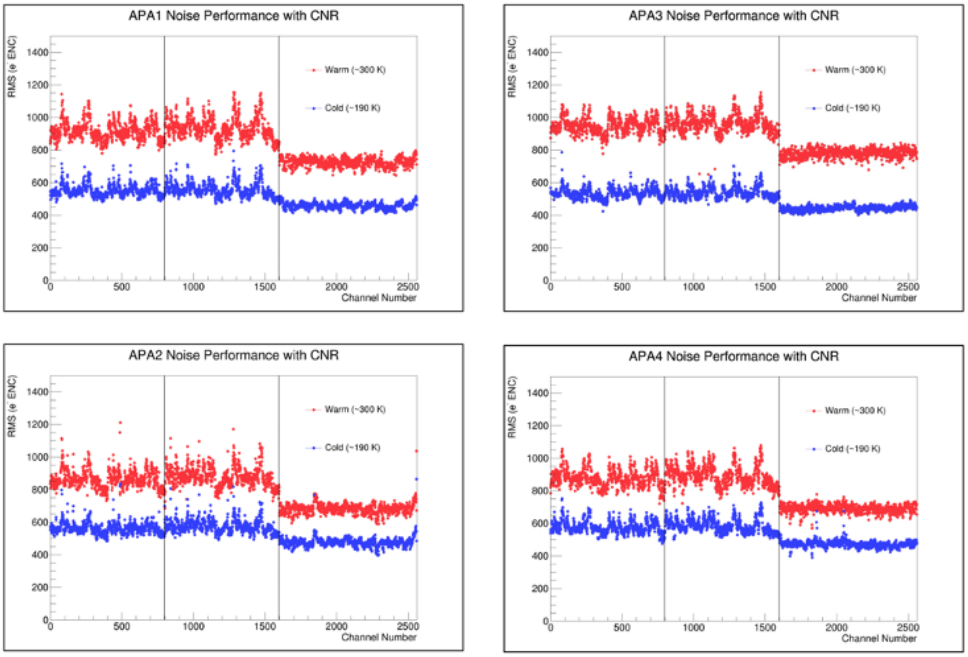

Figure 10: The first 1600 channels of each APA plot are the induction channels, the last 960 are collection channels. The collection channels have an overall lower noise because of their lower wire capacitance. The induction channels also have somewhat higher natural variation in their noise because different induction channels have different total wire capacitance due to the way they wrap around the APA. Collection channel noise is more uniform because of the same wire capacitance.

The production of the photon detectors for ProtoDUNE-SP mirrored the full production chain that will be employed in FD1-HD. The 7680 SiPMs were produced by FBK and Hamamatsu photonics and instrument 40 modules. The SiPM boards were tested in Bologna and Ferrara using the mass test facility of FD1-HD ("CACTUS"). The failure rate for SiPM production corresponds to 0.08%. Since each PDS module comprises four electronic channels ("supercell"), each supercell was tested in standalone mode in CIEMAT and Milano Bicocca before the module assembly at CERN (see Fig.12). After assembly, each module was tested at room temperature using a dark box equipped with a LED system. After installation inside the APA, the modules were tested in the cold box. No failure has been reported at the temperature of the cold box (about 170 K) except for one disconnected supercell due to a faulty APA connector (APA2 module 8 channel 4). The cold box runs were employed to validate the DAPHNE boards, too. The analog part of DAPHNE was improved during the tests both at CERN and in Milano Bicocca (DAPHNE v2) and achieved excellent performance. Photon detectors integrated into the APA's, have shown very good behavior during the cold test and no electric interference with the APA cold electronics was observed. Cables have been pulled through the penetration and connected to the flanges on top of the cryostat in September 2022.

Temperature sensors located inside the APAs frame and around the cryostat structure have been successfully connected to the DCS. The purity monitor system has been reassembled with the refurbished detectors and tested. It will be kept under vacuum and installed in the cryostat just before the filling with LAr to avoid the exposure of the detector to air during a long period.

Both the drift volumes have been completed and the field cage closed The second and last drift on the Jura side was successfully closed by November 2022 (Fig.13).

The laser beam location detectors, a subsystem of the Ionization Laser system, have been also installed in the cryostat and tested. The Ionization Laser System installation procedures have been successfully validated in December 2022 by inserting the periscopes into the cryostat from the associated

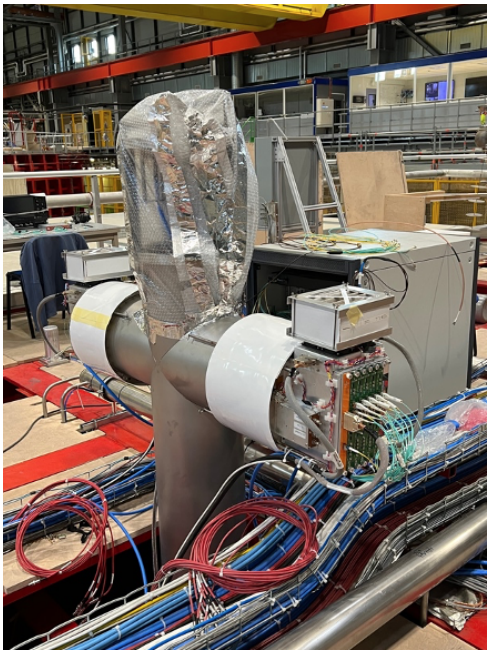

Figure 11: The Warm Interface Boards receiving the cold electronics signals, installed on the roof of the NP04 cryostat. The CE cables have been pulled through cryostat penetration and connected to the WIB's the via the cryostat feedthroughs.

penetrations (see Fig. 11b). At the end of the exercise, the system has been removed. In fact, both the Cryogenics Instrumentation (Purity monitors, Temperature monitors and Cameras) and the Ionization Laser system will be installed just before the cryostat filling to avoid leaving them in air for a long period.

Most of the ProtoDUNE installation procedures worked fine, only few needed some adjustments. Thanks to the ProtoDUNE-II experience, they have been all validated for the DUNE Far Detector 1.

The new beam plug (Fig. 4) has been installed and positioned between the upstream end wall of the Salève side and the cryostat tertiary membrane; the survey to fine tune the alignment has been completed in mid-November 2022 (Fig.14).

A broken wire in the bottom APA3 (the last APA installed) was discovered by visual inspection after its installation inside the cryostat. The wire has been successfully removed and the broken pieces have been analyzed with the electronic microscope. The data analysis on the signals from the APA3 wires showed that the wire disconnected during the warming up after the cold test in October 2023. This incident is being studied in detail. No final report is available yet, but it looks that most probably the wire suffered from some mechanical stresses. The APA3 was tested after the wire removal. The wire planes are correctly isolated from each other. No excess noise is detected in any channel. The APA is fully functional and ready for the filling.

At the end of the the LAr-TPC installation, the TCO was covered with a polyethylene sheet to protect the detector from dust. The present plan is to close the TCO by summer 2023. The TCO closure with the proper insulation layers will last 5 weeks and it could start in July 2023 or later depending on the availability of the LAr. Once this is done, the Cryogenic Instrumentation and the Ionization Laser system monitor detectors will be installed, the cryostat sealed and filled with Gaseous Ar to avoid any detector deterioration while waiting for the filling with LAr. It will take about 3 weeks to install the missing detectors on the roof of the cryostat, do the last checks inside the cryostat and close all the penetrations on the roof. It will then take about 1 week to purge the cryogenics lines and fill the detector with Gaseous Ar. Therefore, we foresee that the cryostat will be ready to be filled with LAr by Autumn 2023.

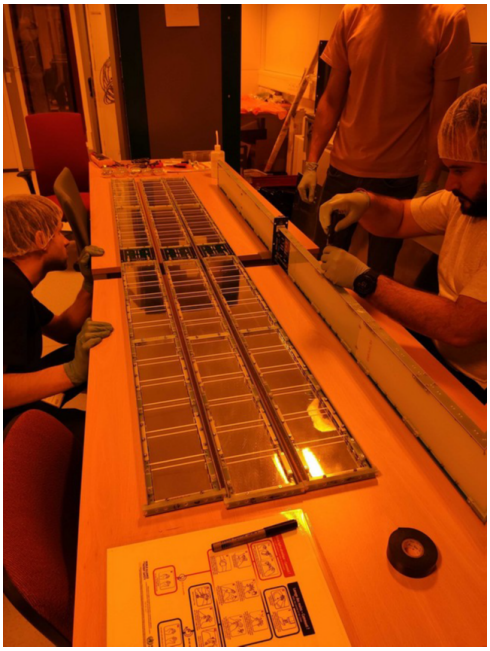

Figure 12: Assembly of supercells into PDS modules at CERN.

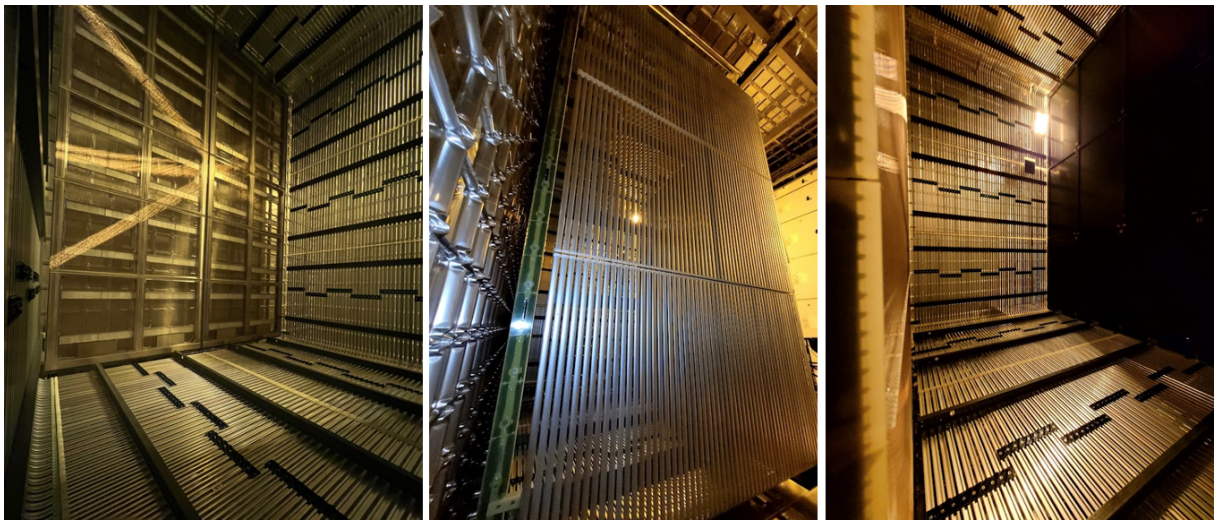

Figure 13: Views the LAr-TPC (APA, Cathode and Field cage), after the deployment of the top and bottom field cage modules and the positioning of the FC end walls. No relevant issues with the alignment of the TPC components were encountered.

In parallel, the repositioning of the CRT and the re-installation of the beam line and the trigger counters will take 3 weeks and can be planned once the beam time schedule is known.

Finally, the LAr filling is foreseen to take about 5 weeks. Therefore, if the TCO closure is concluded in the summer 2023, the NP04 detector could be operational toward the end of 2023. The availability in 2023 of the required argon amount (approximately 850 ton) will be known at the latest by June. A tentative schedule highlighting the main tasks required to enable NP04 operation is presented in Fig.15.

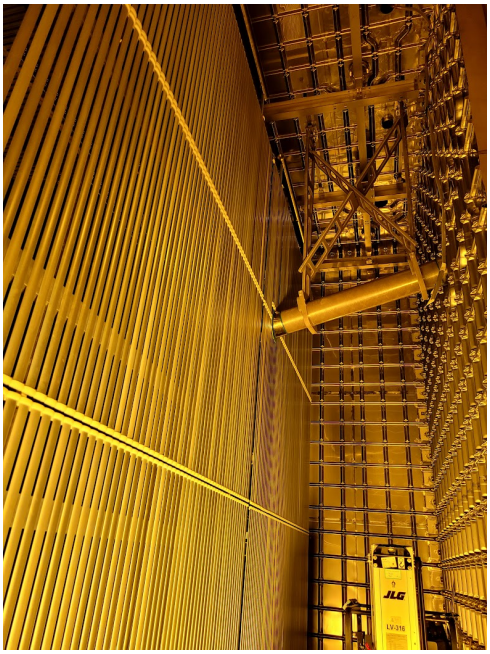

Figure 14: View of the 1.8 m long (250 mm diameter) beam plug installed between the cryostat membrane and the upstream Field Cage end Wall (Salève side). The inclination reflects the alignment with respect to the beam line; a survey for alignment fine tuning has been performed at the end of 2022.

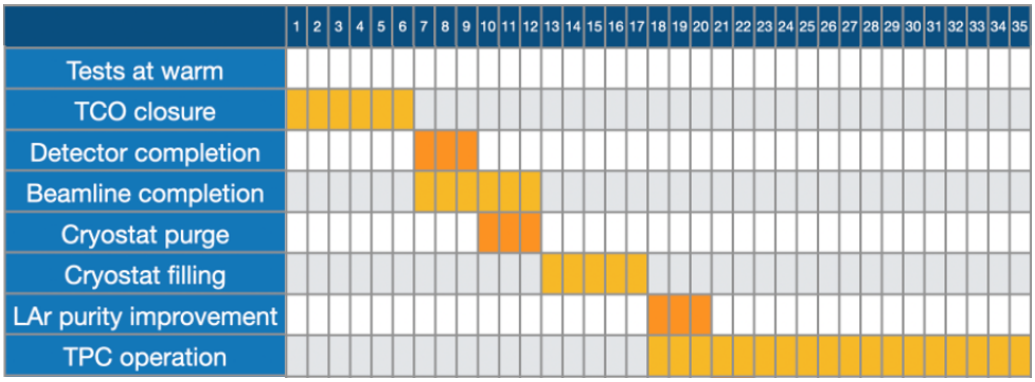

Figure 15: Tentative schedule towards NP04 operation in case of availability of LAr. Week 1 is when TCO closure starts.

2.2 Status and plans for commissioning and calibration

The procurement process to purchase 850 ton of liquid argon required to fill NP04 (and subsequently NP02) started in spring 2022. As of today, none of the major European companies dealing with cryogenic liquids engages in a contract. The procurement of liquid argon in Europe is, at the moment, still uncertain: price and delivery time are undefined. We explored the possibility of delivery liquid argon from the US and running cryogenic plants for a dedicated LAr production. These alternatives are prohibitive due to high costs. In the past years, the availability of argon increased during summertime. We aim therefore at receiving the liquid argon within fall 2023. It is to be noticed that, at that time, also the vertical drift module0 will be completed in NP02; this opens the possibility to fill first either NP04 or, optionally, NP02. This possibility is under discussion within the DUNE collaboration, which is aware of the implications that this decision would have on the beam line and beam instrumentation.

For the upcoming operation, NP04 is instrumented with a different time projection chamber(TPC)

with respect to NP04 Phase I. The biggest change is the reduction by 1/3 in the length of the TPC (nearly along the incident beam direction). In preparation for the analysis cosmic rays and beam data, the simulated geometry has been modified to reflect this new layout. Some modifications still remain to be implemented in this geometry – namely the active optical readout components and the new "beam plug" which displaces some of the liquid argon between the cryostat and the TPC volume. These will be completed soon and will be followed by the production of a large Monte Carlo (MC) sample; initial analysis will follow.

In addition to the structural components of the simulated geometry, the change in the active TPC volume will result in a different magnitude of space charge effect (SCE) in the TPC. A simulation of this SCE has been completed, and full implementation into the simulation/analysis software is in the works. Finally, MC event generators for two new calibration systems – 1) a periscopic laser system and 2) a pulsed neutron source – are needed. The first of these is nearly fully integrated into simulation software, while preparation/design of the second has begun.

The DAQ system is fully integrated with the charge readout electronics of NP04, and it has been used for the individual testing of the detector components in the cold-box runs. The electronics of the four Anode Plane Assemblies installed in the cryostat is read out through the DAQ to carry out regular noise runs and to monitor the stability of the detectors. The integration with the new DAPHNE boards to readout the photon detection system is progressing well, and the integration with the LED calibration system is complete. Work is planned in summer 2023 to re-integrate the CRT system.

In 2022 the DAQ baseline design for the DUNE readout evolved from FELIX to 100G Ethernet, allowing to transition towards commercially available components, thus eliminating the need for custom production of electronics. The trigger chain, which originally was planned to be partially within FELIX card's gateware, is now fully implemented in software, leveraging efficient programming techniques, such as Single Instruction Multiple Data (SIMD) processing. The data driven trigger has been successfully exercised at NP04 using artificial pulsing of CE channels.

After several months of development and testing in laboratory setups, in close collaboration with the CE experts, the integration work to upgrade the NP04 system to the new readout started. Two of the APAs installed in the cryostat have been already successfully connected to the Ethernet chain. The transition will be completed within summer for the charge readout, while the photon detection system will continue being read through FELIX until the end of 2023.

2.3 Plans and Schedule for operation

BE-EA group is informed about the present filling and commission schedule of NP04, and the unavailability of liquid argon until at least the summer of 2023. The installation of the beam platform in front of the TCO and the positioning/activation of the beam instrumentation must follow the TCO closure; this will happen when the liquid argon schedule is better defined. Both the required beam instrumentation and the time and personnel required for its installation is well understood, as it will replicate what was designed and implemented for NP04 Phase-I.

If the beam will be available when the NP04 detector is operational, data with e-, protons, pions, K and mu with momenta between 0.5 Gev/c and 7 GeV/c and positive polarity are still requested with following main goals:

- Benchmark the performance of the LAr TPC
- Evaluation of the long term stability
- Calibrate the TPC with neutrons and low energy (energy) sources
- Events reconstruction and analysis
- Measure hadron-nucleus cross section to reduce systematics

During 2023 and 2024, the cold box in the NP04 clean room will be maintained as a facility for the validation of a fraction of the APA's, constructed in Daresbury (UK), for the DUNE Far Detector 1. The first couple (top bottom) APAs arrived in mid April. They will be equipped with cold electronics and cables and they will go through a full cold box test following the validation procedure strictly developed for the NP04 APA's. After validation, the APA's will be shipped to to storage either in UK or US.

3 Summary

Remarkable progress has been made on the physics analyses, with several papers being produced. In particular, a number of hadronic cross-section analyses are being addressed and have been the subject of new PhD theses.

The Phase II of the experiment has also progressed. The full detector have been installed, allowing to validate most of the procedures defined for the assembly and installation of the DUNE Far Detector 1 components. The current schedule for the TCO closing and the filling with LAr is still driven by the availability of commercial LAr on the market. According to the present tentative schedule, the NP04 detector could be commissioned and made operative by the end of 2023.

A two weeks beam exposure in 2023 was requested earlier this year but, most likely, this request will be postponed to next year. In case of beam exposure, the plan is to collect data to extend the current Phase I π^+ cross section to lower kinetic energies, and to compare with the most well-studied data samples from Phase I and complement it with Negative polarity hadron interactions. Lower energies are also in the plan in case the allocated beam time allows it. Cosmic rays data taking will proceed in parallel to study the overall detector response. Finally a calibration campaign with the ionisation lasers is also in the program.

Bibliography

[1] DUNE collaboration, *Separation of track- and shower-like energy deposits in ProtoDUNE-SP using a convolutional neural network*, *Eur. Phys. J. C* **82** (2022) 903 [2203.17053].

[2] DUNE collaboration, *Identification and reconstruction of low-energy electrons in the ProtoDUNE-SP detector*, 2211.01166.

[3] DUNE collaboration, *Reconstruction of interactions in the ProtoDUNE-SP detector with Pandora*, 2206.14521.

[4] LArIAT collaboration, *Measurement of the (π^-, Ar) total hadronic cross section at the LArIAT experiment*, 2108.00040.

[5] J. Calcutt, *Measurement of π^+ – Argon Absorption and Charge Exchange Interactions Using ProtoDUNE-SP*, Ph.D. thesis, Michigan State U., Michigan State U., 2021.

[6] LADS collaboration, *pi+ absorption on N and Ar*, *Phys. Rev. C* **60** (1999) 054610.

[7] B.K. et al. (The LADS Collaboration), *Pion absorption reactions on n, ar, and xe*, *The European Physical Journal A* **9** (2000) 537.

[8] NOvA collaboration, *New constraints on oscillation parameters from ν_e appearance and ν_μ disappearance in the NOvA experiment*, *Phys. Rev. D* **98** (2018) 032012 [1806.00096].

[9] S.D. et al., *Comparison of validation methods of simulations for final state interactions in hadron production experiments*, *Phys. Rev. D* **104** (2021) 053006 [2103.07535].

[10] M. Strait, *Evaluation of the mean excitation energy of liquid argon*, 2212.06286.

[11] E. Gramellini, *Measurement of the Negative Pion and Positive Kaon Total Hadronic Cross Sections on Argon at the LArIAT Experiment*, Ph.D. thesis, Yale U., 2018. 10.2172/1489387.

[12] T. Adye, *Unfolding algorithms and tests using roounfold*, in *PHYSTAT 2011 Workshop on Statistical Issues Related to Discovery Claims in Search Experiments and Unfolding*, H.B. Prosper and L. Lyon, ed., pp. 313–318, 2011, DOI [1105.1160].

[13] G. D'Agostini, *A multidimensional unfolding method based on Bayes' theorem*, *Nuclear Instruments and Methods in Physics Research Section A: Accelerators, Spectrometers, Detectors and Associated Equipment* **362** (1995) 487.

[14] R. Diurba, *Evaluating the ProtoDUNE-SP Detector Performance to Measure a 6 GeV/c Positive Kaon Inelastic Cross Section on Argon*, Ph.D. thesis, Minnesota U., 2021.

[15] A.C. Booth, N. Charitonidis, P. Chatzidaki, Y. Karyotakis, E. Nowak, I. Ortega-Ruiz et al., *Particle production, transport, and identification in the regime of* $1-7$ GeV/c, *Phys. Rev. Accel. Beams* **22** (2019) 061003.

[16] J. Calcutt and C. Thorpe and K. Mahn and L. Fields, *Geant4Reweight: a framework for evaluating and propagating hadronic interaction uncertainties in Geant4*, *Journal of Instrumentation* **16** (2021) P08042.

[17] S. Agostinelli, J. Allison, K. Amako, J. Apostolakis, H. Araujo, P. Arce et al., *Geant4—a simulation toolkit*, *Nuclear Instruments and Methods in Physics Research Section A: Accelerators, Spectrometers, Detectors and Associated Equipment* **506** (2003) 250.

[18] J. Allison et al., *Geant4 developments and applications*, *IEEE Transactions on Nuclear Science* **53** (2006) 270.

[19] J. Allison et al., *Recent developments in Geant4*, *Nuclear Instruments and Methods in Physics Research Section A: Accelerators, Spectrometers, Detectors and Associated Equipment* **835** (2016) 186.

[20] GENIE Collaboration collaboration, *The GENIE Neutrino Monte Carlo Generator*, *Nucl. Instrum. Meth. A* **614** (2010) 87 [0905.2517].

[21] C. Andreopoulos, C. Barry, S. Dytman, H. Gallagher, T. Golan, R. Hatcher et al., *The GENIE neutrino Monte Carlo generator: Physics and user manual*, *arXiv preprint* (2015) [1510.05494].

[22] GENIE collaboration, *Neutrino-Nucleon Cross-Section Model Tuning in GENIE v3*, 2104.09179.

[23] GENIE collaboration, *Hadronization model tuning in genie v3*, *Phys. Rev. D* **105** (2022) 012009 [2106.05884].

[24] S. Dytman, Y. Hayato, R. Raboanary, J.T. Sobczyk, J. Tena Vidal and N. Vololoniaina, *Comparison of validation methods of simulations for final state interactions in hadron production experiments*, *Phys. Rev. D* **104** (2021) 053006 [2103.07535].

[25] J.H. Parker Jr and J.J. Lowke, *Theory of electron diffusion parallel to electric fields. i. theory*, *Physical Review* **181** (1969) 290.

[26] ICARUS collaboration, *Performance of a three-ton liquid argon time projection chamber*, *Nuclear Instruments and Methods in Physics Research Section A: Accelerators, Spectrometers, Detectors and Associated Equipment* **345** (1994) 230.

[27] Y. Li, T. Tsang, C. Thorn, X. Qian, M. Diwan, J. Joshi et al., *Measurement of longitudinal electron diffusion in liquid argon*, *Nuclear Instruments and Methods in Physics Research Section A: Accelerators, Spectrometers, Detectors and Associated Equipment* **816** (2016) 160 [1508.07059].

[28] ICARUS collaboration, *Electron diffusion measurements in the icarus t600 detector*, in *Journal of Physics: Conference Series*, vol. 888, p. 012060, IOP Publishing, 2017, DOI.

[29] DarkSide-50 collaboration, *Electroluminescence pulse shape and electron diffusion in liquid argon measured in a dual-phase tpc*, *Nuclear Instruments and Methods in Physics Research Section A: Accelerators, Spectrometers, Detectors and Associated Equipment* **904** (2018) 23 [1802.01427].

[30] MicroBooNE collaboration, *Measurement of the longitudinal diffusion of ionization electrons in*

the microboone detector, *Journal of Instrumentation* **16** (2021) P09025 [2104.06551].

[31] MINOS collaboration, *Observation of Seasonal Variation of Atmospheric Multiple-Muon Events in the MINOS Near and Far Detectors*, *Phys. Rev. D* **91** (2015) 112006 [1503.09104].

[32] R. Antolini et al., *Seasonal variations in the underground muon intensity as seen by macro*, *Astroparticle Physics* **7** (1997) 109.

[33] NOvA collaboration, *Seasonal variation of multiple-muon cosmic ray air showers observed in the NOvA detector on the surface*, *Phys. Rev. D* **104** (2021) 012014 [2105.03848].

[34] Daya Bay collaboration, *Seasonal Variation of the Underground Cosmic Muon Flux Observed at Daya Bay*, *JCAP* **01** (2018) 001 [1708.01265].

[35] OPERA collaboration, *Measurement of the cosmic ray muon flux seasonal variation with the OPERA detector*, *JCAP* **10** (2019) 003 [1810.10783].